Lindland, K. P., and S. G. Terjesen, "The Effect of a Surface-Active Agent on Mass Transfer in Falling Drop Extraction," *Chem. Eng. Sci.*, **5**, 1 (1956).
Mayfield, F. W., and W. L. Church, Jr., "Liquid-Liquid Extractor Design," *Ind. Eng. Chem.*, **44**, 2253 (1952).
Meister, B. J., and G. F. Scheele, "Generalized Solution of the Tomotika Stability Analysis for a Cylindrical Jet," *AIChE J.*, **13**, 682 (1967).
———, "Prediction of Jet Length in Immiscible Liquid Systems," *ibid.*, **15**, 689 (1969).
Minhas, S. S., "Dispersed Phase Mass Transfer During Drop Formation and Coalescence in Liquid-Liquid Extraction," Ph.D. dissertation, Univ. Notre Dame, Ind. (1969).
Perry, R. H., C. H. Chilton, and S. D. Kirkpatrick, *Chemical Engineer's Handbook*, 4 ed., McGraw-Hill, New York (1963).
Rayleigh, Lord, "On the Instability of Jets," *Proc. London Math. Soc.*, **10**, 4 (1879).
———, "On the Capillary Phenomena of Jets," *Proc. Royal Soc. (London)*, **29**, 71 (1879).
Reddy, K. A., and L. K. Doraiswamy, "Estimating Liquid Diffusivity," *Ind. Eng. Chem. Fundamentals*, **6**, 77 (1967).
Sawistowski, H., "Influence of Mass-Transfer-Induced Marangoni Effects on Magnitude of Interfacial Area and Equipment Performance in Mass Transfer Operations," *Chem. Ingr. Tech.*, **45**, 1114 (1973).
Scheele, G. F., and B. J. Meister, "Drop Formation at Low Velocities in Liquid-Liquid Systems: Part I. Prediction of Drop Volume. Part II. Prediction of Jetting Velocity," *AIChE J.*, **14**, 9 (1968).
Sherwood, T. K., R. L. Pigford, and C. R. Wilke, *Mass Transfer*, p. 188, McGraw-Hill, New York (1975).
Siemes, W., and J. F. Kauffman, "Tropfenbildung in Flüssigkeiten an Düsen bei hohen Durchsätzen," *Chem. Ingr. Tech.*, **29**, 32 (1957).
Skelland, A. H. P., *Diffusional Mass Transfer*, Chapt. 8, Wiley-Interscience, New York (1974).
———, and W. L. Conger, "A Rate Approach to Design of Perforated-Plate Extraction Columns," *Ind. Eng. Chem. Process Design and Develop.*, **12**, 448 (1973).
Skelland, A. H. P., and K. R. Johnson, "Jet Break-up in Liquid-Liquid Systems," *Can. J. Chem. Eng.*, **52**, 732 (1974).
Skelland, A. H. P., and S. S. Minhas, "Dispersed Phase Mass Transfer during Drop Formation and Coalescence in Liquid-Liquid Extraction," *AIChE J.*, **17**, 1316 (1971).
Skelland, A. H. P., and R. M. Wellek, "Resistance to Mass Transfer inside Droplets," *ibid.*, **10**, 491, 789 (1964).
Smith, S. W. I., and H. Moss, "Experiments with Mercury Jets," *Proc. Royal Soc. (London)*, **A93**, 373 (1917).
Tomotika, S., "On the Instability of a Cylindrical Thread of a Viscous Liquid surrounded by Another Viscous Fluid," *ibid.*, **A150**, 322 (1935).
Treybal, R. E., *Liquid Extraction*, pp. 467-8, McGraw-Hill, New York (1963).
Tyler, E., and E. G. Richardson, "The Characteristic Curves of Liquid Jets," *Proc. Phys. Soc. (London)*, **37**, 297 (1925).
Tyler, E., and F. Watkin, "Experiments with Capillary Jets," *Phil. Mag.*, **14**, 849 (1932).
Vermeulen, T., "Theory for Irreversible and Constant-Pattern Solid Diffusion," *Ind. Eng. Chem.*, **45**, 1664 (1953).
Weber, C., "Disintegration of a Liquid Jet," *Z. Angew Math. Mech.*, **11**, 136 (1931).

Manuscript received February 17, 1977; revision received May 16, and accepted May 27, 1977.

Elongational Flow Behavior of Viscoelastic Liquids:

Part I. Modeling of Bubble Collapse

A spherically collapsing gas bubble will create a uniaxial extension of the fluid surrounding it. This flow may be readily analyzed, and it is possible to relate observed experimental parameters such as the pressure inside the bubble and the bubble collapse rate to the predictions of viscoelastic constitutive relations. This study compares the predictions of the Newtonian fluid and a viscoelastic model to observed bubble collapse in three fluids: one Newtonian fluid and two viscoelastic polymer solutions. Good agreement between data and the model was observed for the Newtonian experiments. The viscoelastic solutions, however, yielded rates of collapse which were greater than the Newtonian predictions based on equal zero-shear viscosity. Subsequent modeling with a modified corotational Maxwell fluid yielded good agreement with the data for the transient elongational response in the viscoelastic solutions.

GLEN PEARSON
and
STANLEY MIDDLEMAN
Department of Chemical Engineering
University of Massachusetts
Amherst, Massachusetts 01003

SCOPE

The behavior of viscoelastic fluids in elongation is of special importance in such industrial processes as fiber spinning, blow molding, vacuum forming, tubular film extrusion, and certain coating and calendering operations. To date, very little is known about the behavior of viscoelastic fluids in elongation. A particular void exists for fluids of moderate viscosity ($\eta_o \sim 10^2 - 10^4$ *P*) and at high rates of strain ($\dot{\epsilon} > 1\ s^{-1}$).

Correspondence concerning this paper should be addressed to Stanley Middleman. Glen Pearson is with Eastman Kodak Company, Rochester, New York 14650.

The goal of this study is to develop a method for observing the response of polymer solutions and low viscosity melts to an elongational deformation which may be readily analyzed with existing viscoelastic constitutive relations. If we use the elongational flow induced by a collapsing gas bubble in a fluid of interest, valuable information concerning the transient elongational behavior of such fluids can be obtained. Comparison of this elongational behavior to the predictions of various constitutive models can then be used to discriminate among models which are otherwise indistinguishable on the basis of shear experiments alone.

CONCLUSIONS AND SIGNIFICANCE

The use of bubble collapse is a viable means to study the elongational flow behavior of polymer solutions and low viscosity melts. The flow has the added advantage of being easily analyzed in terms of existing fluid constitutive models so that observable system parameters may be related to predictions of these models. It is hoped that the results of this study will lead to more work of a similar nature with fluids which are well defined in a macromolecular sense, so the results may be compared to and used in conjunction with the several available molecular and entanglement constitutive models.

The modern rheologist, and the polymer process designer, rely heavily on data obtained from simple shear or viscometric flow instruments in an attempt to predict the behavior of polymeric fluids in industrially important flows. Many commercial processes, however, involve deformations which are quite unlike those attained in viscometric instruments, and hence these processes are not well described by parameters obtained through viscometric, simple shear experiments.

It is important, then, to be able to achieve well-defined deformations other than simple shear not only from the viewpoint of industrial applications, but also because the behavior of materials in flows other than simple shear can shed light on the nature of the deformation process in materials. This is particularly true in the attempt of rheologists to write relatively simple, yet reasonably complete, constitutive equations for viscoelastic fluids. Among a variety of constitutive equations proposed for polymeric fluids, many lead to identical predictions for behavior under viscometric conditions. This type of degeneracy can be removed, in some cases, through the study of nonviscometric flows.

One such nonviscometric flow, which is of considerable importance industrially, is the extensional or elongational flow. Middleman (1968) defines such flows in terms of the rate of deformation tensor $\mathbf{\Delta}$. A uniaxial elongational flow may be defined by a velocity field

$$u = [u_1(x_1), 0, 0] \tag{1}$$

and

$$\mathbf{\Delta} = \dot{\epsilon} \begin{bmatrix} 2 & 0 & 0 \\ 0 & -1 & 0 \\ 0 & 0 & -1 \end{bmatrix} \tag{2}$$

The elongational viscosity is defined as the ratio of the primary normal stress difference $\tau_{11} - \tau_{22}$ to the elongation rate $\dot{\epsilon}$:

$$\eta_e = \frac{\tau_{11} - \tau_{22}}{\dot{\epsilon}} \tag{3}$$

Inherent to the definition of viscosity is that Equation (3) only apply to steady state kinematics and dynamics. Dealy (1971) offers a review of several other types of elongational flows.

A variety of industrial processes involve elongational flows. These include fiber spinning, blow molding, vacuum forming, tubular film extrusion, and certain types of coating and calendering operations. Despite its industrial importance, relatively little has been achieved in the study of elongational flow. A major obstacle has been the design of a well-defined experiment. This has been particularly true with regard to relatively low viscosity fluids, say shear viscosities less than 10^4 poise, and thus most polymer solutions and molten polymers of importance have not been examined with respect to their elongational behavior. Indeed, relatively little data exist at all for any fluids.

The goal of the work described herein is the development of an experimental system, and the requisite theoretical modeling, to allow quantitative determination of elongational behavior in solutions of polymers and in low viscosity molten polymers. Specifically, the task set is to study the collapse of spherical bubbles of air within the fluids of interest. Spherical bubble collapse creates a uniaxial elongational flow. It will be demonstrated that it is possible to determine both the kinematics and the dynamics of this flow and hence to utilize this information in a study of the elongational rheology of relatively low viscosity polymeric fluids. This paper considers only certain aspects of the theoretical study and presents illustrative transient data. A more detailed study, including several models of the transient elongational behavior and a complete compilation of data, is given in Pearson (1976). The transient results will be interpreted in terms of elongational viscosity behavior in subsequent communications.

REVIEW OF RELATED STUDIES

Owing to the importance of elongational flow, industrially and rheologically, there has been considerable activity towards experimentally determining elongational behavior for a variety of polymeric fluids. Principally, a great deal of effort has been focused on techniques which might measure elongational viscosity as a function of strain rate, much as the cone and plate experiment measures the viscometric functions. There are two classes of experiments which have been successful in this endeavor, both using very high viscosity polymer melts ($\eta_o > 10^6$ poise) at relatively low rates of strain ($\dot{\epsilon} < 10^{-1}$ s^{-1}). While there have been two very good reviews of the literature (Dealy, 1971; Cogswell, 1975), it is instructive to summarize the major results of past experiments in order to put the present work in proper perspective.

The rod pulling experiments form the first class. Following the work of Trouton (1906) who studied Newtonian materials, the behavior of several polymer melts has been investigated. Most of the studies conclude that η_e is relatively insensitive to strain rate as exemplified by the work of Ballman (1965) and Vinogradov et al. (1972) for poly-

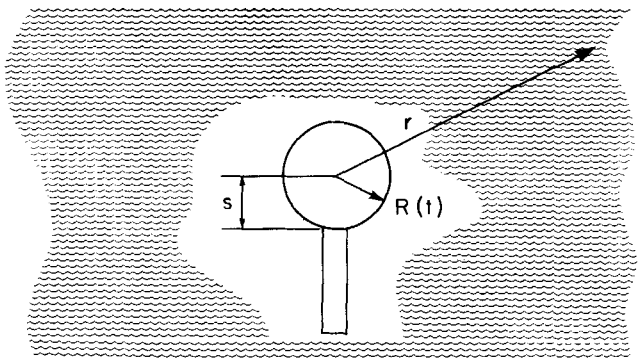

Fig. 1. Bubble geometry for a single spherical bubble surrounded by an infinite sea of fluid.

styrene, Vinogradov et al. (1970) for polyisobutylene, Stevenson (1972) for an isobutylene-isoprene copolymer, and Cogswell (1969) for polymethylmethacrylate. More recently, Peng and Landel (1974) and Bailey (1974), both using polyisobutylene, find a decrease of η_e with increasing strain rates.

Contrasted to the work on polyisobutylene is that of Cogswell (1969) and Meissner (1972), who both indicate that for low density polyethylene, the elongational viscosity increases with strain rate. Meissner's work with the rotational clamp comprises a set of transient elongations at constant strain rate. The interpretation that η_e increases with strain rate comes from the fit of the transient stress by the Lodge Rubberlike Liquid (Chang and Lodge, 1972).

A second major class of experiments successfully used to measure elongational viscosity is based on the work of Denson and Gallo (1971) concerning bubble inflation. The inflation of a hemispherical bubble can be used to study the biaxial elongation of a polymer melt of high viscosity. For polyisobutylene, η_{eb} (the biaxial elongational viscosity) decreases with increasing elongation rate. Maerker and Schowalter (1974) have shown it is possible to use lower viscosity materials, again polyisobutylene, and achieve strain rates approaching 1 s^{-1}. They observe first a slight decrease in η_{eb} and then an increase with strain rate.

Several other methods have been used in attempts to measure elongational behavior with less success than the two mentioned above. The principal problems have been attainment of steady state stress and strain rate in a Lagrangian sense and creation of a well-defined flow field. Among the more promising methods proposed is the rotating drop technique of Hsu and Flumerfelt (1975). Based on a method for determining interfacial tension developed by Princen (1967), a drop of the fluid to be studied is carefully placed along the axis of a cylinder containing an immiscible Newtonian fluid of lower viscosity and higher density. The cylinder is then rotated about its axis in a manner programmed to produce the desired strain behavior.

Obviously, a reliable technique should be developed for studying elongational flow behavior over as wide a range of strain rates as possible. In particular, a need exists to use lower viscosity materials as well as higher strain rates than is possible with either the tensile testing (rod pulling) apparatus or the bubble inflation method of Denson. In developing such a technique, it is important to include a complete mathematical treatment of the transient aspects of the flow. Consideration of elongational flow transients is desirable not only because of the difficulty of designing steady state experiments, but also because the industrial flow fields, for which the knowledge of fluid behavior is desired, are rarely of a steady state nature.

THEORY

An example of simple elongational flow is presented by the inflation or collapse of a spherical gas bubble completely surrounded by fluid. If, as in Figure 1, we imagine a bubble of gas surrounded by a sea of fluid of interest, then collapse of the bubble in a spherically symmetric manner will create a uniaxial elongational flow in the fluid.

In order to obtain rheological information for the fluid, the kinematic and dynamic variables must be related to measurable experimental parameters. The kinematics are completely specified by the continuity equation for incompressible materials which leads directly to

$$u_r = f(t)/r^2 = R^2\dot{R}/r^2 \tag{4}$$

as the only nonzero component of the velocity vector. The second part of Equation (4) follows from knowing that the bubble wall velocity [at $r = R(t)$] is $\dot{R} = dR/dt$. From Middleman (1968), the rate of deformation tensor in spherical coordinates is

$$\mathbf{\Delta} = \begin{bmatrix} 2\dfrac{\partial u_r}{\partial r} & 0 & 0 \\ 0 & 2\dfrac{u_r}{r} & 0 \\ 0 & 0 & 2\dfrac{u_r}{r} \end{bmatrix} \tag{5}$$

The rate of deformation tensor for the fluid surrounding the bubble is then given by Equation (2), with

$$\dot{\epsilon} = -2R^2\dot{R}/r^3 \tag{6}$$

The dynamics of the system are governed by conservation of momentum in the radial direction

$$\rho\left(\frac{\partial u_r}{\partial t} + u_r\frac{\partial u_r}{\partial r}\right) = -\frac{\partial p}{\partial r} + [\nabla\cdot\tau]_r \tag{7}$$

where

$$[\nabla\cdot\tau]_r = \frac{1}{r^2}\frac{\partial}{\partial r}(r^2\tau_{rr}) - \frac{\tau_{\theta\theta}+\tau_{\phi\phi}}{r} \tag{7a}$$

Replacing the velocity in Equation (7) with Equation (4) and integrating from the bubble wall to infinity, one finds that Equation (7) becomes

$$\rho\left(RR + \frac{3}{2}R^2\right) = P_L - P_\infty + \int_R^\infty [\nabla\cdot\tau]_r\,dr \tag{8}$$

Equation (8) is a general form of Rayleigh's equation (Lamb 1945) when the fluid is considered to exert a finite stress due to motion.

The fluid pressure P_L at the bubble surface can be related to the more easily measured pressure inside the bubble P_G by accounting for the continuity of normal stress at the bubble wall:

$$-P_G + \tau^G{}_{RR} = -P_L + \tau^L{}_{RR} - \frac{2\sigma}{R} \tag{9}$$

The pressure P_G is the average gas pressure within the bubble if we assume complete homogeneity in the gas phase. Since $\tau^G{}_{RR}$ represents the dynamic stress due to a gas of low viscosity, it may be safely neglected.

Upon substituting for P_L in Equation (8), one finds that the equation describing bubble deformation becomes

$$\rho\left(\dot{R}\dot{R} + \frac{3}{2}\dot{R}^2\right) = P_G - P_\infty - \frac{2\sigma}{R} + 2\int_R^\infty \frac{\tau_{rr}-\tau_{\theta\theta}}{r}\,dr \tag{10}$$

Table 1. Material Functions for the MZFD Fluid [(Equation (18)]

$$\eta = \frac{\eta_0}{(1 + a\lambda\dot{\gamma})^m(1 + (\lambda_{ef}\dot{\gamma})^2)}$$

$$\psi_{12} = \frac{2\lambda\eta_0}{(1 + (\lambda_{ef}\dot{\gamma})^2)(1 + a\lambda\dot{\gamma})^m(1 + \lambda\dot{\gamma})}$$

$$\eta_e = \frac{3\eta_0}{(1 + a\lambda\sqrt{3}\dot{\epsilon})^m}$$

where $$\lambda_{ef} = \frac{\lambda}{1 + \lambda\sqrt{\frac{1}{2}II_\Delta}}$$

In obtaining Equation (10), angular symmetry was used to evaluate the divergence of the stress field in the radial direction.

By substituting into Equation (10) the constitutive relationship between deviatoric stress and deformation, one can then describe elongational flow surrounding the bubble for any type of fluid. In some instances, Equation (10) leads directly to a prediction of bubble radius as a function of time. Such is the case for the generalized Newtonian fluid (GNF), defined by

$$\boldsymbol{\tau} = \eta\boldsymbol{\Delta} \tag{11}$$

where η is a scalar function of the first three invariants of the rate of deformation tensor $\boldsymbol{\Delta}$:

$$\eta = \eta(I_\Delta, II_\Delta, III_\Delta) \tag{12}$$

In practice, since $I_\Delta = 0$ for incompressible fluids, and since there are no precedents for including III_Δ, we shall specify η as a function only of II_Δ. One can easily see that the GNF reduces to the Newtonian fluid if the viscosity is independent of the rate of deformation.

Because the fluids used in this study are fairly viscous ($\eta_0 \sim 10^3$ P), inertial effects will be neglected. The magnitude of system and fluid parameters such that inertia may be ignored for Newtonian materials has been previously estimated (Pearson, 1974). From Equation (10), then, we find in the absence of inertia

$$P_G - P_\infty - \frac{2\sigma}{R} = -2\int_R^\infty \frac{\tau_{rr} - \tau_{\theta\theta}}{r}\,dr \tag{13}$$

For the GNF, it is evident that incompressibility implies that $tr(\boldsymbol{\tau}) = 0$, so

$$\tau_{rr} - \tau_{\theta\theta} = 3/2\,\tau_{rr} \tag{14}$$

and

$$P_G - P_\infty - \frac{2\sigma}{R} = -3\int_R^\infty \frac{\tau_{rr}}{r}\,dr \tag{15}$$

Substituting the constitutive relation [Equation (11)] into Equation (15) and integrating by parts, we get

$$-\tau_{RR} = P_G - P_\infty - \frac{2\sigma}{R} - 4R^2\dot{R}\int_R^\infty \frac{\partial\eta/\partial r}{r^3}\,dr \tag{16}$$

where τ_{RR} is the radial normal stress at the bubble wall, which is related to the bubble strain rate by

$$\tau_{RR} = -4\eta\frac{\dot{R}}{R} \tag{17}$$

Thus, if η is given as a function of II_Δ, then the integral in Equation (16) will be some function of $R(t)$, and Equation (16) will be an integro-differential equation for $R(t)$, the solution of which will depend upon $P_G(t)$ and, of course, the parameters that appear in the constitutive equation. The applicability of any generalized Newtonian fluid model to transient elongational flow can then be tested.

It is desirable to be able to evaluate Equation (13) with viscoelastic as well as with purely viscous constitutive forms. One useful model of viscoelasticity may be obtained by a slight modification of the Zaremba-Fromm-Dewitt (ZFD) fluid discussed by Bird and his co-workers (1974). Analogous to the White-Metzner fluid, allow the ZFD fluid to become

$$\tau^{ij} + \lambda_{ef}\frac{\mathcal{D}\tau^{ij}}{\mathcal{D}t} = \eta_{ef}\Delta^{ij} \tag{18}$$

where

$$\frac{\mathcal{D}\tau^{ij}}{\mathcal{D}t} = \frac{\partial\tau^{ij}}{\partial t} + u_k\frac{\partial\tau^{ij}}{\partial x_k} + 1/2(\omega^{im}\tau^{mj} - \omega^{mj}\tau^{im}) \tag{19}$$

$$\lambda_{ef} = \frac{\lambda}{1 + \lambda\sqrt{1/2\,II_\Delta}} \tag{20}$$

$$\eta_{ef} = \frac{\eta_0}{[1 + a\lambda\sqrt{1/2\,II_\Delta}]^m} \tag{21}$$

[We note that bubble collapse creates an irrotational flow, for which the components of $\boldsymbol{\omega}$ in Equation (19) vanish identically.] The material functions for this model are given in Table 1. The method used to choose the material constants is discussed in the appendix. Of particular significance is the fact that this model predicts η_e to be a decreasing function of strain rate.

In spherical coordinates the stress difference $\tau_{rr} - \tau_{\theta\theta}$ is given by

$$\frac{\partial(\tau_{rr} - \tau_{\theta\theta})}{\partial t} + \frac{R^2\dot{R}}{r^2}\frac{\partial(\tau_{rr} - \tau_{\theta\theta})}{\partial r} + \frac{\tau_{rr} - \tau_{\theta\theta}}{\lambda_{ef}} = \frac{-4\eta_{ef}}{\lambda_{ef}}\frac{R^2\dot{R}}{r^3} \tag{22}$$

This partial differential equation may be reduced to an ordinary differential equation by applying the following coordinate transformation

$$t \rightarrow t' \tag{23}$$

$$1/3\,[r^3 - R^3(t)] \rightarrow \xi \tag{24}$$

due to Epstein and Plesset (1950) and later used by Street (1968), Fogler and Goddard (1970), Zana and Leal (1975), and Ting (1975) in problems similar to this one. The resulting expression for stress is

$$\frac{d(\pi_{\xi\xi} - \pi_{\theta\theta})}{dt'} + \frac{\pi_{\xi\xi} - \pi_{\theta\theta}}{\lambda_{ef}} = \frac{-4\eta_{ef}}{\lambda_{ef}}\frac{R^2\dot{R}}{3\xi + R^3} \tag{25}$$

where the θ coordinate is unchanged in the transformation, and π^{ij} represents the deviatoric stress in the new coordinate system. Equation (13) in the new coordinate system becomes

$$P_G - P_\infty - \frac{2\sigma}{R_oY} = -2\int_o^\infty \frac{\pi_{\xi\xi} - \pi_{\theta\theta}}{3\xi + R_o^3Y^3}\,d\xi \tag{26}$$

For a given strain program, Equations (25) and (26) may be integrated numerically to yield predictions of the time dependent bubble pressure function Φ, which we define as

$$\Phi = P_G - P_\infty - \frac{2\sigma}{R_oY} \tag{27}$$

The exact details of this integration are available elsewhere (Pearson, 1976).

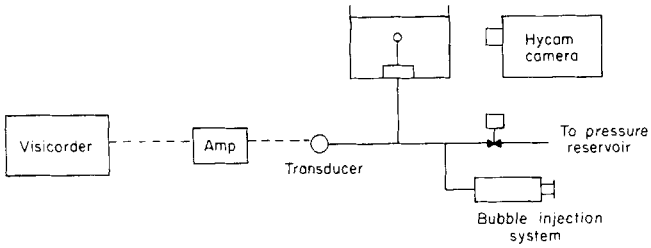

Fig. 2. Typical equipment setup for experimentation.

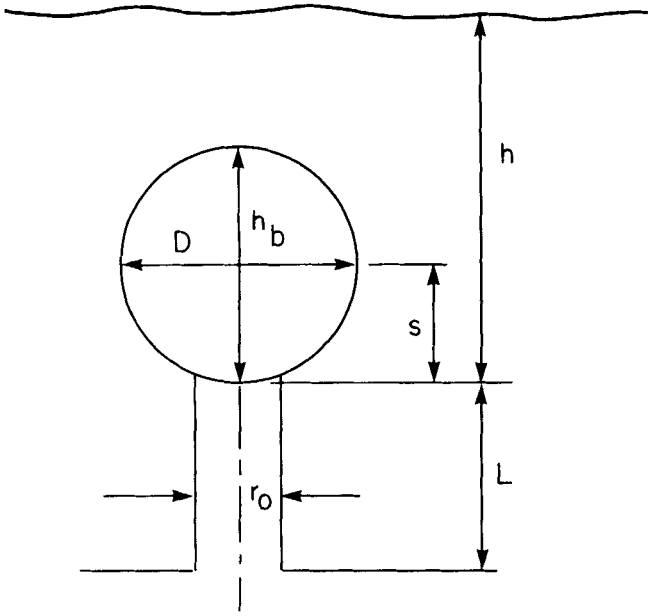

Fig. 3. Sketch of typical experimental bubble shape showing dimensions needed for the data analysis.

EXPERIMENTAL

The experimental apparatus used for studying bubble collapse is shown schematically in Figure 2. The bubble was supported by a Teflon® capillary in an acrylic box, roughly 10 cm³. Capillaries were available in several sizes ranging from 0.04572 to 0.269 cm I.D. with 0.1194 cm being used most frequently. The camera used to film the bubble motion was a high speed 16 mm motion picture camera capable of filming at speeds of 300 to 900 frames/s.

The collapse of the bubble was controlled in this set of experiments by the pressure applied to the bubble after it had been initially formed. The simplest form of pressure program is a step change. The bubble prior to collapse is stationary with an equilibrium pressure P_o balancing hydrostatic and surface tension effects. At $t = 0$, the solenoid valve is energized, which applies a constant pressure P_R from the reservoir. For collapse, P_R is less than P_o. Pressure in the reservoir was measured with a differential manometer. Typical reservoir pressures were between 0 and 5 cm of water gauge. All runs were made at constant reservoir pressure conditions.

Before a filming session, the particular fluid studied is placed in the sample box with a positive pressure supplied to the capillary by a standard syringe pump, keeping the capillary free of fluid and also serving to saturate the solution with air. At the start of a run, the reservoir pressure P_R is set and several test bubbles are injected with a small 2 cm³ syringe to test for conditions of collapse at the chosen value of P_R and bubble size. Once the proper conditions are obtained, a final bubble is injected and brought to rest atop the capillary. At this point, one starts the camera and allows sufficient time for full speed to be developed before energizing the solenoid valve to an open condition. Filming continues until the bubble collapses entirely.

Table 2. Physical Properties of the Polymer Solutions Studied

Fluid composition	Silicone oil pure	PA* 0.98% (wt) in 50/50 glycerine/water	HPC† 2.0% (wt) in water
$[M_v]$	—	$>10^6$	7.4 (10^5)
ρ(g/cm³)	1.136	1.115	1.004
σ(dyne/cm)	23.6	62.2	41.8
$\eta_0(p)$ @ 25°C	344	2 240	620

* PA = polyacrylamide.
† HPC = hydroxypropylcellulose.

After the film is processed, the data of bubble radius and height of its center above the capillary as a function of time are taken from frame by frame projection of the film on a flat wall. Typical magnification ratios are generally twenty five or more. Timing of the bubble sequence is achieved with an independent timing light generator which places a dot on the film every 0.01 s.

The final step in processing the data is calculating effective spherical radii and relating reservoir pressure to the pressure inside the bubble. As in the work of Szekely and Fang (1971), we found it necessary, owing to slightly nonspherical bubble shapes, to use an average radius defined as

$$R = (D + h_b)/2 \tag{28}$$

where D and h_b are the diameter and the height of the bubble above the capillary, respectively.

The bubble pressure P_G may be evaluated by referring to Figure 3. With the bubble stationary, just prior to the start of an experiment, P_G is

$$P_G = -P_h \tag{29}$$

where P_h is the average hydrostatic pressure at the bubble center $\rho g(h - s)$, s being the center height. At $t = 0$, the bubble experiences a step change in pressure. If there were no pressure loss, then $P_G = P_o - P_h$. However, as Szekely and Fang have noted, P_G in general will differ from P_o by an amount ΔP_L due to a pressure drop in the small capillary. Using a quasi steady state analysis

$$\Delta P_L = \frac{8\mu_{AIR}L}{\pi r_o^4} Q(t) \tag{30}$$

where L and r_o are capillary dimensions, μ_{AIR} the viscosity of air, and $Q(t)$ the flow rate which may be directly related to the bubble volume change with time, $4\pi R^2\dot{R}$. The magnitude of this pressure drop is small for the collapse runs considered here and has been neglected. The magnitude of ΔP_L can be significant for bubble growth, particularly when the bubble radius becomes large.

Experiments were performed with three fluids: a silicone oil, a solution of polyacrylamide in water and glycerine (PA), and a solution of hydroxypropylcellulose in water (HPC). For characterization purposes, density, surface tension, and viscometric data were necessary. Since the fluids were moderately viscous, surface tension was measured by the pendant drop technique. Table 2 shows the values obtained for density and surface tension as well as the solution composition for the three fluids. Viscometric data, consisting of the shear viscosity, first normal stress difference, and dynamic viscosity are shown in Figures 4,

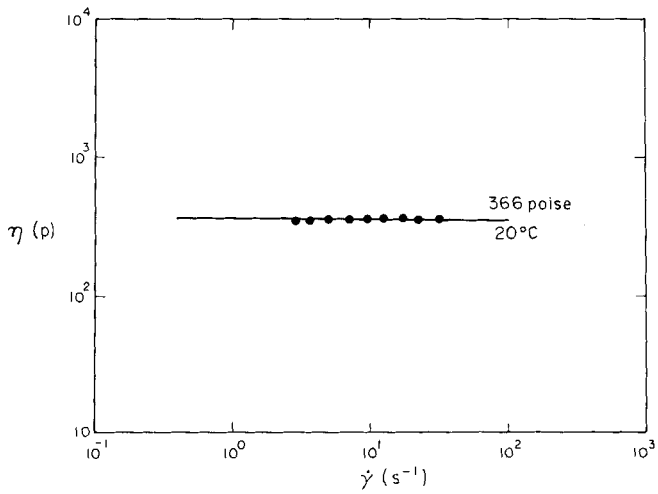

Fig. 4. Shear viscosity of silicone oil at 20°C.

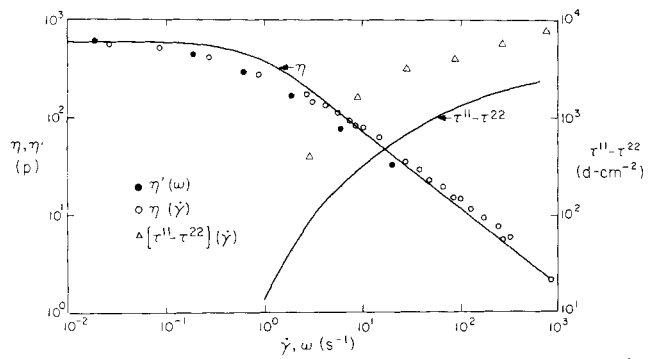

Fig. 5. Viscosity, normal stress difference, and dynamic viscosity for the hydroxypropylcellulose solution. Curves correspond to modified ZFD fluid with parameters from Table 3.

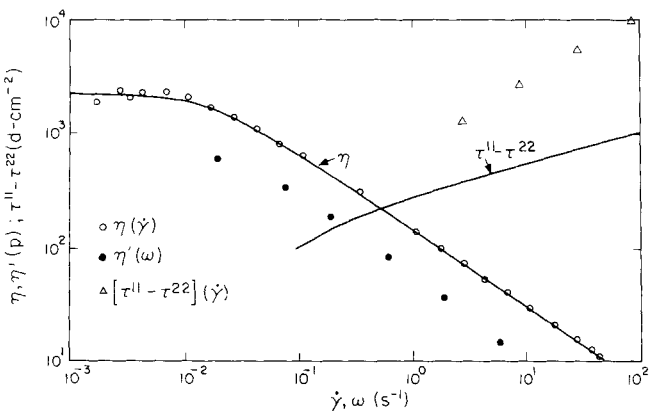

Fig. 6. Viscosity, normal stress difference, and dynamic viscosity for the polyacrylamide solution. Curves correspond to modified ZFD fluid with parameters from Table 3.

5, and 6. Only shear viscosity data are given for the silicone oil, since it was found to be a Newtonian fluid.

RESULTS AND DISCUSSION

The first tests were made with silicone oil, chosen since it may be modeled as a Newtonian fluid. The physical assumptions used in deriving the basic model of bubble collapse could then be checked using a simple fluid constitutive relation. From Equation (15), for a Newtonian fluid, the bubble radius as a function of time is found to be the solution to

$$\frac{\dot{Y}}{Y} = \frac{P_G - 2\sigma/R_oY}{4\eta_o} \tag{31}$$

TABLE 3. MATERIAL CONSTANTS FOR THE MZFD FLUID

	HPC	PA
$\eta_0(p)$	620.0	2240.0
$\lambda(s)$	0.48	66.0
a	0.76	0.32
m	1.5	0.70

where $Y = R/R_o$ is a normalized bubble radius. For the experiment described above, P_G is given by

$$P_G = P_o - P_h = P_o - \rho g(h - s) \tag{32}$$

(P_∞ is used as the reference pressure atmospheric).

A typical run for silicone oil is shown in Figure 7. The agreement between the model and data is encouraging and justifies the assumptions made in modeling the process.

Figure 8 shows experimental data for bubble radius as a function of time for two runs in the HPC solution compared to the predictions of the Newtonian model. It is obvious that for this viscoelastic fluid the Newtonian model is not adequate to predict fluid response. Furthermore, the use of a purely viscous model with parameters selected to fit shear viscosity data does not yield an appreciably better representation of the collapse data. Hence, modeling with viscoelastic constitutive relations is examined.

Owing to the nature of the experiment, that is, pressure step change, an initial condition on stress is necessary for solution of the equations for the viscoelastic fluid. We have found that the particular initial condition chosen has little effect upon the predictions for $\Phi(t)$ (Pearson, 1976), so we assume that at $t = 0^+$, the stress distribution from the bubble wall to ∞ is identical to a Newtonian distribution

$$\pi_{\xi\xi} = \frac{\pi_{\xi\xi}|_{\xi=0,\,t=0^+}}{3\xi + R^3} \tag{33}$$

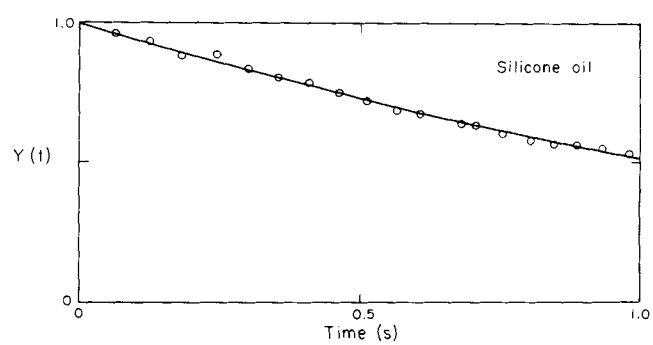

Fig. 7. Comparison of bubble collapse data for silicone oil to Equation (31) describing collapse in a Newtonian fluid.

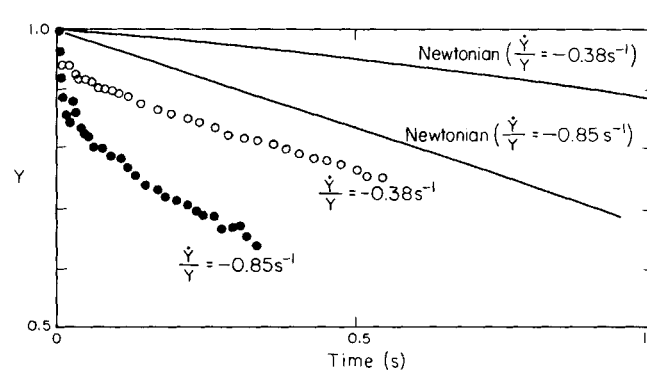

Fig. 8. Prediction of Y (t) using the Newtonian fluid model compared to data for the HPC solution.

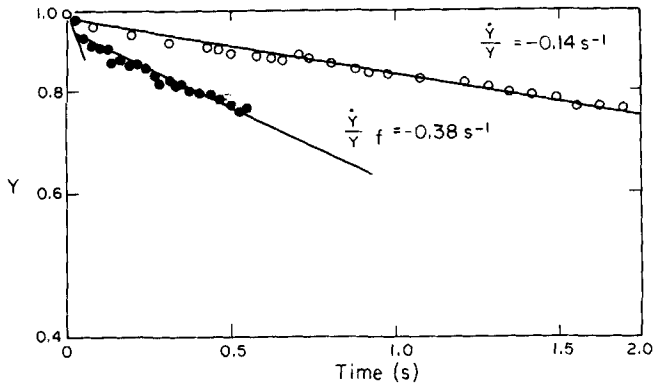

Fig. 9. Semilogarithmic plot of $Y(t)$ vs. time showing constant strain rate conditions obtained for the HPC solution.

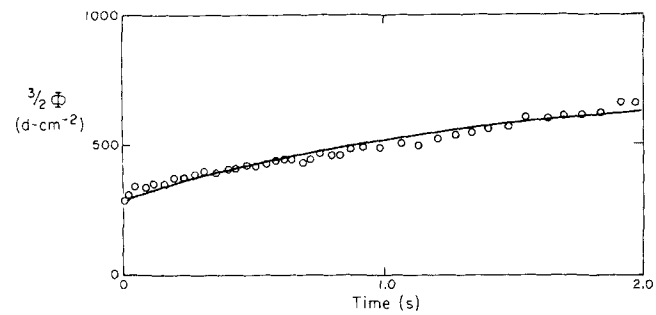

Fig. 11. Experimental data for 3/2 $\Phi(t)$ vs. time compared to the prediction of the modified ZFD fluid for the HPC solution, $\dot{Y}/Y = -0.14\ s^{-1}$.

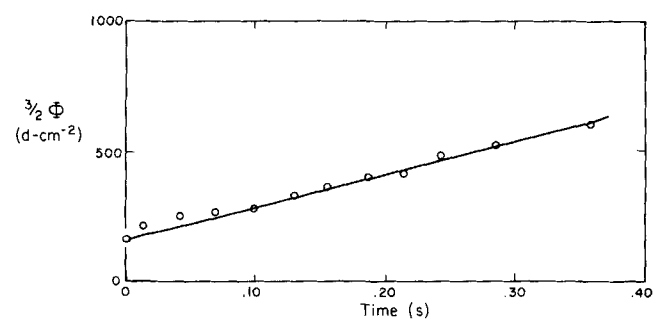

Fig. 13. Experimental data for 3/2 $\Phi(t)$ vs. time compared to the predictions of the modified ZFD fluid for the PA solution, $\dot{Y}/Y = -0.82\ s^{-1}$.

$$\pi_{\theta\theta} = \frac{-1/2\pi_{\xi\xi}|_{\xi=0,\,t=0^+}}{3\xi + R^3} \tag{34}$$

where

$$\pi_{\xi\xi}|_{\xi=0,\,t=0^+} = -\frac{3}{2}[P_o - \rho g(h-s) - 2\sigma/R_o] \tag{35}$$

Figures 9 and 10 show data for bubble radius as a function of time for runs in both the HPC and the PA solutions. Also shown are the fit of these data with simple exponential forms which are readily substituted into Equations (25) and (26) and integrated to give predictions of $\Phi(t)$. One should note that this experiment does yield constant strain rate data.

The result of this integration is shown in Figures 11 to 14 compared to experimental data at various strain rates. It is seen that the modified ZFD model follows the observed elongational flow behavior quite well with the material constants as given in Table 3. Of particular importance is that all the fluid material parameters were chosen from viscometric (shear) data, and, as shown in Figures 5 and 6, the model gives a good representation of shear data as well.

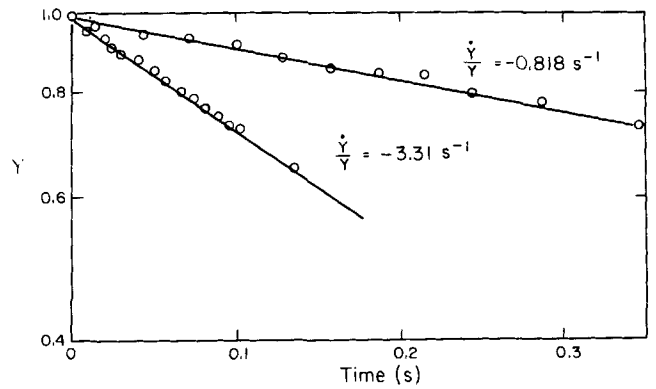

Fig. 10. Semilogarithmic plot of $Y(t)$ vs. time showing constant strain rate conditions obtained for the PA solution.

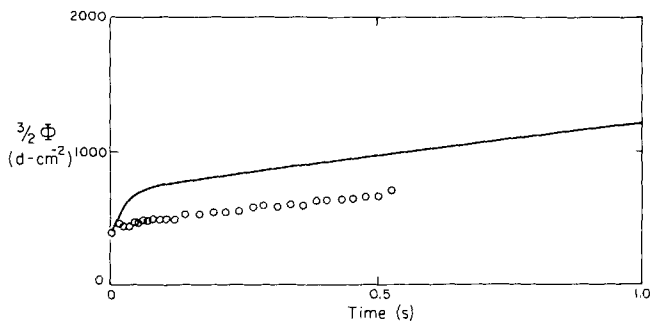

Fig. 12. Experimental data for 3/2 $\Phi(t)$ vs. time compared to the predictions of the modified ZFD fluid for the HPC solution, $\dot{Y}/Y = -0.38\ s^{-1}$.

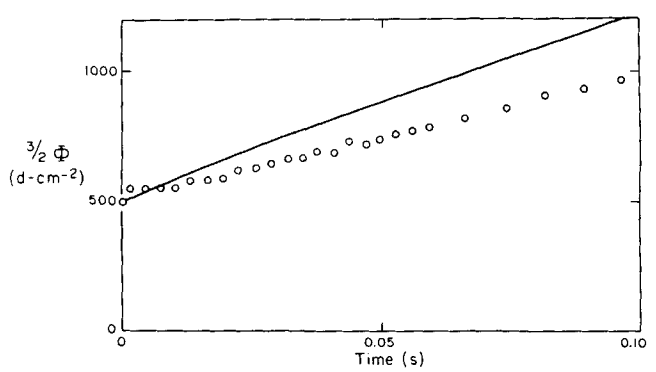

Fig. 14. Experimental data for 3/2 $\Phi(t)$ vs. time compared to the predictions of the modified ZFD fluid for the PA solution, $\dot{Y}/Y = -3.31\ s^{-1}$.

One is led to speculate, from the agreement obtained using the modified ZFD model to fit transient elongational stress data, that the elongational viscosity for the two polymer solutions studied decreases with strain rate. Further support of this speculation comes from comparing the stress data to predictions of viscoelastic models which lead to increasing $\eta_e(\dot{\epsilon})$. We found these models (Pearson, 1976) in all cases to give significantly poorer fits of the transient data. The transient data, in several cases, are at high enough strain rates that the difference between predictions of stretch thinning and stretch thickening models is significant.

ACKNOWLEDGMENT

This work was supported by the National Science Foundation under Grant GK 41899. This support is gratefully acknowledged. We also wish to thank Professor Roger Tanner of the University of Sydney and Professor R. Byron Bird of the University of Wisconsin for their assistance and time in discussing this work.

NOTATION

a = material parameter of GNF fluid, s
D = bubble diameter, cm
g = acceleration due to gravity, cm-s^{-2}
h = height of fluid above capillary base, cm
h_b = height of bubble top above capillary, cm
L = length of capillary, cm
m = material parameter of GNF
p, P = pressure, dyne-cm^{-2}
P_h = average hydrostatic pressure at bubble center, dyne-cm^{-2}
P_R = reservoir pressure, dyne-cm^{-2}
P_o = equilibrium pressure, dyne-cm^{-2}
$Q(t)$ = volume flow rate of air through capillary, cm^3-s^{-1}
r_o = capillary inside radius, cm
$R(t)$ = bubble radius, cm
$\dot{R}, \ddot{R}$ = time derivatives of bubble radius, cm-s^{-1}, cm-s^{-2}
s = bubble center height above capillary, cm
t, t' = time variable, s
u = velocity, cm-s^{-1}
x = general coordinate direction, cm
Y = normalized bubble radius

Greek Letters

α = parameter of Rouse spectrum
$\dot{\gamma}$ = shear rate, s^{-1}
$\mathbf{\Delta}$ = rate of deformation tensor
$\dot{\epsilon}$ = strain rate, s^{-1}
η = viscosity function for the GNF, p
η_e = elongational viscosity, p
η_{eb} = biaxial elongational viscosity, p
η_{ef} = effective viscosity for MZFD fluid, p
λ = relaxation time, s
λ_{ef} = effective relaxation time for the MZFD fluid, s
μ_{AIR} = viscosity of air, p
ξ = coordinate direction in the moving coordinate system, cm^3
π = stress tensor in moving coordinate system, dyne-cm^{-2}
ρ = density, g-cm^{-3}
σ = surface tension, dyne-cm^{-1}
τ = stress tensor, dyne-cm^{-2}
Φ = bubble pressure function, dyne-cm^{-2}
ω = vorticity tensor = $[\nabla u - (\nabla u)^T]$

Roman Letters

I_Δ, II_Δ, III_Δ = principal invariants of the rate of deformation tensor

Superscripts and Subscripts

$\left\{\begin{matrix}1, & 2, & 3\\ r, & \theta, & \phi\end{matrix}\right\}$ coordinate direction
G = quantity measured on the gas side of the bubble
L = quantity measured on the liquid side of the bubble
∞ = quantity measured at a point far from the bubble surface

LITERATURE CITED

Bailey, F. D., "New Extensional Viscosity Measurements on Polyisobutylene," *Trans. Soc. Rheol.*, **18**, 635 (1974).

Ballman, R. L., "Extensional Flow of Polystyrene Melt," *Rheol. Acta.*, **4**, 137 (1965).

Bird, R. B., O. Hassager, and S. I. Abdel-Khalik, "Co-rotational Rheological Models and the Goddard Expansion," *AIChE J.*, **20** 1041 (1974).

Chang, H., and A. S. Lodge, "Comparison of Rubberlike-Liquid Theory with Stress Growth Data for Elongation of a Low Density Branched Polyethylene Melt," *Rheol. Acta.*, **11**, 127 (1972).

Cogswell, F. N., "Tensile Deformations in Molten Polymers," *ibid.*, **8**, 187 (1969).

———, "Polymer Melt Rheology During Elongational Flow," paper presented at the American Chemical Society Symposium on Fiber and Yarn Processing at Philadelphia, Pa. (Apr., 1975).

Dealy, J. M., "Extensional Flow of Non-Newtonian Fluids—A Review," *Polym. Eng. Sci.*, **11**, 433 (1971).

Denson, C. D., and R. J. Gallo, "Measurements on the Biaxial Extensional Viscosity of Bulk Polymers: The Inflation of a Thin Polymer Sheet," *Polym. Eng. Sci.*, **11**, 174 (1971).

Epstein, P. S., and M. S. Plesset, "On the Stability of Gas Bubbles in Liquid—Gas Solution," *J. Chem. Phys.*, **18**, 1505 (1950).

Hsu, J., and R. Flumerfelt, "Rheological Applications of a Drop Elongation Experiment," *Trans. Soc. Rheol.*, **19**, 523 (1975).

Fogler, H. S., and J. D. Goddard, "Collapse of Spherical Cavities in Viscoelastic Fluids," *Phys. Fluids*, **13**, 1135 (1970).

Lamb, H., *Hydrodynamics*, Dover Publications, New York (1932).

Maerker, J. M., and W. R. Schowalter, "Biaxial Extension of an Elastic Liquid," *Rheol. Acta.*, **13**, 627 (1974).

Meissner, J., "Development of a Universal Extensional Rheometer for the Uniaxial Extension of Polymer Melts," *Trans. Soc. Rheol.*, **16**, 405 (1972).

Middleman, S., *The Flow of High Polymers*, Interscience, New York (1968).

Pearson, G., Ph.D. dissertation, Univ. Mass., Amherst (1976).

———, and S. Middleman, "Comments on a New Method for Determination of Surface Tension of Viscous Liquids," *Chem. Eng. Sci.*, **29**, 1051 (1974).

Peng, S-T. J., and R. F. Landel, "Response of Bulk Polymer Under Motion with Constant Stretch Histories," *Rheol. Acta.*, **13**, 548 (1974).

Princen, H. M., "Measurement of Interfacial Tension from the Shape of a Rotating Drop," *J. Colloid Interfacial Sci.*, **23**, 99 (1967).

Spriggs, T. W., "A Four Constant Model for Viscoelastic Fluids," *Chem. Eng. Sci.*, **20**, 931 (1965).

Stevenson, J. F., "Elongational Flow of Polymer Melts," *AIChE J.*, **18**, 540 (1972).

Street, J. R., "The Rheology of Phase Growth in Elastic Liquids," *Trans. Soc. Rheol.*, **12**, 103 (1968).

Szekely, J., and S-D Fang, "On Bubble Formation at the Tip of a Capillary with Downward Gas Flow," *Chem. Eng. Sci.*, **26**, 1123 (1972).

Ting, R. Y., "Viscoelastic Effect of Polymers on Single Bubble Dynamics," *AIChE J.*, **21**, 810 (1975).

Trouton, F. T., "On the Coefficient of Viscous Traction and its Relation to that of Viscosity," *Proc. Royal Soc. London*, **A77**, 426 (1906).

———, B. V. Raduskevich, and V. D. Fikhman, "Extension of Elastic Liquids—Polyisobutylene," *J. Polymer Sci.*, **8**, Part A-2 (1970).

Vinogradov, G. V., V. D. Fikhman, and B. V. Raduskevich, "Uniaxial Extension of Polystyrene at True Constant Stress," *Rheol. Acta.*, **11**, 286 (1972).

Zana, E., and L. G. Leal, "Dissolution of a Stationary Gas Bubble in a Quiescent, Viscoelastic Fluid," *Ind. Eng. Chem. Fundamentals*, **14**, 175 (1975).

APPENDIX

The modified Zaremba-Fromm-Dewitt fluid has four material constants, all readily determined from a combination of steady and small amplitude sinusoidal shear data. The zero shear viscosity η_0 is the linear viscoelastic limit for both η' and η. The relaxation time λ may be obtained in a number of ways. For this work, we assume that λ is identical to the maximum relaxation time from the Rouse theory. Many constitutive relations reduce to an identical form for $\eta'(\omega)$:

$$\eta'(\omega) = \sum_{n=1}^{\infty} \frac{\eta_n}{1 + (\lambda_n \omega)^2} \qquad \text{(A1)}$$

Substituting a Rouse spectrum (Spriggs, 1965) into Equation (A1)

$$\lambda_n = \lambda_n^{-\alpha} \tag{A2}$$

$$\eta_n = \eta_o \lambda_n \Big/ \sum_{n=1}^{\infty} \lambda_n \tag{A3}$$

one obtains

$$\eta' = \frac{\eta_o}{Z(\alpha)} \sum_{n=1}^{\infty} \frac{p^\alpha}{p^{2\alpha} + (\lambda\omega)^2} \tag{A4}$$

where $Z(\alpha)$ is the Riemann Zeta function. The relaxation time λ is readily obtained from Equation (A4) by a master curve technique.

The final two fluid constants m and a are determined from steady shear viscosity data. The power law slope of the viscosity-shear rate curve is m, while a is obtained again by a master curve technique.

Manuscript received October 8, 1976; revision received July 6, and accepted July 7, 1977.

Part II. Definition and Measurement of Apparent Elongational Viscosity

The collapse of a single spherical gas bubble within a large body of fluid creates a uniaxial elongational flow in the surrounding fluid. Collapse under constant bubble pressure is observed to produce nearly constant strain rate kinematics. If the steady state stress at the bubble/fluid boundary could be measured, it would be possible to estimate the elongational viscosity of the fluid.

Unfortunately the experiment does not yield the desired stress data, except in the special case of the Newtonian fluid. We are led to define an apparent elongational viscosity, and for specific constitutive models we can evaluate the deviation between the apparent and true viscosity. The experimental and theoretical work indicate that the apparent elongational viscosity provides a good estimate of true elongational viscosity for the two viscoelastic solutions studied so far.

SCOPE

The standard techniques for measuring elongational viscosity work only for highly viscous melts ($\eta_o > 10^6$ *P*) and at low strain rates ($\dot{\epsilon} < 10^{-1}$ s^{-1}). In many cases of practical importance in the polymer processing industry, it is desirable to have elongational flow information for concentrated polymer solutions or low molecular weight polymer melts, both of which exhibit modest viscosities. As well, elongational behavior at higher strain rates must be studied.

Collapse of a single spherical gas bubble in a sea of fluid will create a uniaxial extensional flow. For two concentrated polymer solutions of moderate viscosity ($\eta_o \sim 10^3$ *P*), constant strain rates of 10^{-1} to 10 s^{-1} were achieved. Through evaluation of the transient elongational flow behavior, one can determine if the fluid studied exhibits stretch thickening or stretch thinning elongational viscosity. Assuming the latter, we present an evaluation of an apparent elongational viscosity as a function of strain rate for two solutions. The assumption that the fluids are stretch thinning is consistent with the data.

CONCLUSIONS AND SIGNIFICANCE

The bubble collapse experiment can be used to estimate the elongational viscosity of a concentrated polymer solution. The actual measurement is of an apparent elongational viscosity $\eta_{e,\text{app}}$. A comparison of $\eta_{e,\text{app}}$ data to the predictions of the Tanner-Simmons Rupture model and the modified corotational (Zaremba-Fromm-DeWitt) Maxwell model was made, with good agreement exhibited for both viscoelastic solutions studied. The constitutive test was severe in that all material constants were fit using viscometric (shear flow) data prior to predicting $\eta_e(\dot{\epsilon})$.

Part I of this paper dealt with certain aspects of the transient response of a viscoelastic fluid to an elongational flow (Pearson and Middleman, 1977). The collapse of a spherical gas bubble surrounded by an infinite sea of fluid was analyzed using both purely viscous and viscoelastic constitutive models. Experiments were performed with Newtonian and viscoelastic solutions of moderate viscosity ($\eta_o \sim 1\,000$ *P*). Collapse of the bubble was induced by a rapid change of pressure within the bubble. From measurement of bubble pressure, and high-speed photography of bubble collapse, the dynamics and kin-

Correspondence concerning this paper should be addressed to Stanley Middleman. Glen Pearson is with Eastman Kodak Company, Rochester, New York 14650.